Short Communication

Study on Structural and Optical Properties of Wurtzite Cu₂ZnSnS₄ Nanocrystals Synthesized via Solvothermal Method

Zohreh Shadrokh[1,*], Ahmad Yazdani[2] and Hosein Eshghi[1]

[1]Department of Physics, Shahrood University of Technology, P.O. Box 316-36155, Shahrood, Iran.
[2]Department of Physics, Tarbiat Modares University, P.O. Box 14115-175, Tehran, Iran.

(*) Corresponding author: shadrokhzohreh@gmail.com

Abstract

A simple low-cost solvothermal method was applied to synthesize hexagonal wurtzite Cu₂ZnSnS₄ (CZTS) nanoparticles with different morphologies using Polyvinylpyrrolidone (PVP) as a capping ligand and copper and zinc acetate salts at 180 and 220 ℃. The resulting sphere-like and flower-like nanoparticles synthesized at 180 and 220℃, respectively, indicated thecalculated optical band gaps of 1.45 and 1.28 eV, respectively. Where both samples indicated the metastable wurtzite phase. The main Raman peaks were observed at 333 and 371 cm⁻¹, was indicating the wurtzite phase of CZTS nanocrystals. The phase of the wurtzite CZTS nanoparticles was successfully controlled by using zinc acetate salt, which affected the reaction rate between Zn and S sources. In addition, reaction temperature was found as an effective factor on the morphology, elemental ratio, reaction kinetic, crystallinity, and size of the CZTS nanoparticles. Photoresponse of the CZTS thin films were confirmed by I-V measurements under dark and light illumination. All these results imply the potential of these nanoparticles for solar cell applications.

Keywords: *Semiconductors, Wurtzite CZTS nanoparticles, Solvothermal method, Raman spectroscopy.*

1. INRODUCTION

Cu-based ternary and quaternary chalcogenides such as $CuIn(S,Se)_2$ (CIS), $CuIn_xGa_{1-x}(S,Se)_2$ (CIGS), and Cu_2ZnSnS_4 (CZTS) are promising materials for thin-film solar cells because of their high absorption coefficients as well as direct and optimal energy band gap ranging from 1.4 to 1.6 eV. Among these materials, CZTS has received a greater attention because of its non-toxicity and containing earth-abundant low-cost elements (Zn, Sn)[1-4]. To prepare CZTS nanocrystals, there are many simple stoichiometry-controllable processes and wet chemical methods such as hot-injection [5], microwave-hydrothermal/solvothermal [6], sonochemical [7], and solvothermal [8].

Due to the synthesis process and multistructural nature of the materials, a large number of challenges are confronted to synthesize phase-controllable CZTS nanostructures by the chemical methods such as formation of secondary and ternary phases. Stannite (space group $I\bar{4}2m$), kesterite (space group $I\bar{4}$), and wurtzite (WZ) including WZ stannite ($Pmn2_1$) and WZ kesterite (Pc) are the structures reported for CZTS in either theoretical or experimental works [8-14]. Lu et al. [11] synthesized wurtzite CZTS nanocrystals using the metal chloride, oleylamine (OAm), and oleic acid (OA) as capping agents separately with dodecanethiol

(DDT) as a sulfur source *via* hot injection method. They reported that using the DDT in their work is the key factor for the formation of wurtzite phase, meanwhile OA and OAm assisting in the control of nanocrystals' morphology. Kang et al. [12] reported the aqueous synthesis of WZ CZTS nanocrystals using 3-mercaptopropionic acid (3-MPA) as capping agent and Na_2S as the sulfur source, having a band gap of ~1.43 eV. They claimed Na_2S could produce sulfur anion with a higher reactivity than that of thiourea and, followed by a reaction rate rise at which 3-MPA could reduce the surface energy.

In short, many chemical and thermodynamically parameters such as high reactivity of Cu salt and S source, surfactant (as the capping ligand), solvent, time, temperature, etc. can affect formation of WZ CZTS nanocrystals. By now, phase-controlled synthesis of WZ CZTS still remains a challenge, especially in solvothermal method, so that more studies should be conducted to understand formation mechanism of WZ-CZTS nanocrystals. In the present work, we report influence of temperature on synthesis of quaternary hexagonal WZ CZTS nanoparticles using Cu and Zn acetate salts *via* solvothermal method. The structure, morphology, elemental ratio, and optical and optoelectrical properties of the as-obtained CZTS particles were also studied in this work.

2. EXPERIMENTAL

All of the chemical reagents and solvents were used without further purification and were of analytical grade. Cu $(CH_3Coo)_2$ .H_2O (2 mmol), $Zn(CH_3COO)_2$.$2H_2O$ (1 mmol), $SnCl_2.2H_2O$ (1mmol), Thiourea (TU, 4 mmol), and Polyvinylpyrrolidone (PVP, 0.64 g), were dissolved in 40 mL ethylene glycol (EG) and stirred uniformly. The obtained suspension was transferred into the Teflon container of an autoclave with a volume of 50 ml and held at 180℃

(S1) and 220 ℃ (S2) for 24 hours. The resulting suspension was washed with ethanol and deionized water (DI) (1:3) for three times by centrifuging at 9000 rpm. Finally, the sediment was dried in vacuum at 100 ℃ for 2 hours.

Structural phase and crystalline properties of the samples were examined by X-ray diffraction (XRD) patterns using a diffractometer system (X'Pert Pro MPD) equipped with a Cu-Kα λ=1.5406 Å radiation source, and Raman spectroscopy (SENTERRA, λ=785nm). Absorption spectra were recorded on UNICO (SQ-4802) spectrophotometer. The morphology of the particles was analyzed with Field Emission Scanning Electron Microscopy (FESEM, Zeiss, ∑IJMA-VP). To calculate metal composition and purity of the materials, energy dispersive spectroscopy (EDS) device attached to the FESEM was utilized. Current–voltage (I–V) characteristics of CZTS thin film were measured by using a CHI660B electrochemical workstation under dark and simulated AM 1.5 G spectrum at 100 mW/cm^2 (1sun) illumination, respectively.

3. RESULTS AND DISCUSION

Figure 1a shows the XRD patterns of the as-obtained CZTS particles. The experimental data for these CZTS particles do not completely match with the pattern of zinc blend-derived kesterite phase (JCPDS 26-0575) reported by previous work [1-8, 14]. The main peaks at 2θ = 26.9, 28.5, 30.4, 39.4, 47.4, 51.4, and 56.2° can be attributed to the (100), (002), (101), (102), (110), (103), and (112) planes of the hexagonal wurtzite structure of ZnS. According to the previous reports [9, 11, 13], wurtzite structure of CZTS can be created by substituting Zn with Cu and Sn atoms in WZ ZnS. Moreover, the results of XRD patterns are in good agreements with those reported by the previous works for WZ CZTS [6, 9-11]. As shown in Fig. 1, the peaks labeled by (+) match well with the monoclinic Cu_7S_4 structure.

The presence of these peaks of Cu_7S_4 in S1 sample indicates that the growth process is initiated by the nucleation of Cu_7S_4 because of the high reactivity of Cu with sulfur precursor and WZ CZTS nanocrystals.

We believe that the presence of peaks related to Cu_7S_4 nanocrystals in S1 sample might explain why the reaction temperature is lower than the boiling point
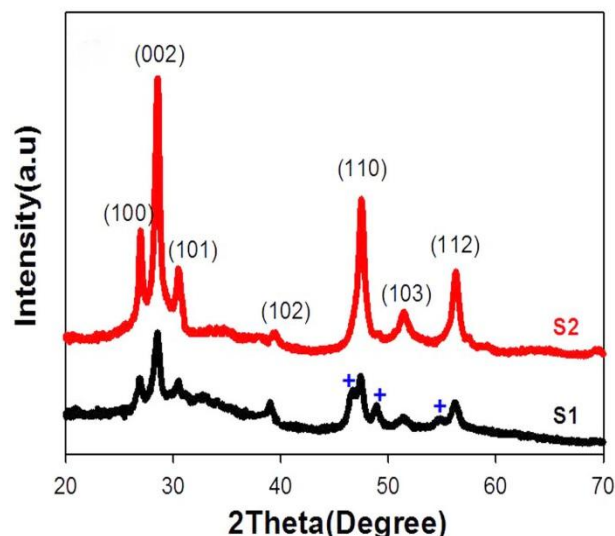

Figure 1. *XRD patterns of WZ CZTS nanoparticles synthesized at 180 ℃ (S1) and 220 ℃ (S2).*

of EG (197 ℃) and why the reaction period is not long enough. Therefore, pressure and energy are not generated enough, and time is not enough, for inter-diffusion of cations between Cu_7S_4 and WZ CZTS nanocrystals. Additionally, XRD pattern of S2 sample shows that the intensity of all peaks increases because of the rise in crystallinity and crystallite size, so almost all Cu_7S_4 peaks eliminate as the reaction temperature increases. Effective crystallite size and strain were calculated from XRD patterns by using the Williamson-Hall formula, also lattice parameters for hexagonal structure can be calculated by using $\frac{1}{d^2} = \frac{4}{3}\left(\frac{h^2+hk+k^2}{a^2}\right) + \frac{l^2}{c^2}$ which d is plane space and h,k,l are Miller indices and a and c are lattice parameters. The results are presented in

Table 1 along with the unit cell volume and lattice constants. The crystallite size increases and strain value decreases because of the drop in grain boundary defects. In addition, the negative strain changes toward the positive values, indicating that the system is under a tensile strain at 220 ℃.

Table 1 *Structural parameters, effective crystallite size and lattice microstrain for S1 and S2 samples.*

Sample	Lattice constant (Å)	V(Å³)	Crystallite size (nm)	ε×10⁻³
S1	a=b=3.838, c=6.314	80.57	7.000	-4.9
S2	a=b=3.837, c=6.288	80.17	21.656	3.6

Moreover, there are also many other similar reports about XRD spectrum and intensity of its main peak [9-11, 15].The considerable point noticed in the study of X-ray diffraction patterns in various reports is the difference between the intensities of the preferred peak at 2θ = 28.5° and the peaks at 27° and 30°. Besides, Regulacio et al. [13], Luo et al. [16], and Sarswat et al. [17] reported that when the intensity of the peak at 2θ = 28.5° is more than those of the adjacent peaks and the peak at 2θ = 33° is observed, the structure is a mix of both phases of zinc blend-derived kesterite and hexagonal wurtzite CZTS. The existence of these various reports indicates the necessity of distinguishing between these two phases from each other. Although, according to the particular position of sulfur in the structure, Raman analysis is able to distinguish wurtzite from kesterite, considering the blue shift (from 337 to 333cm⁻¹) of the main peak of Raman spectrum [9-10, 13-14, 16-17], there still remain ambiguities in this regard.

Figure 2 illustrates the Raman spectrum of the CZTS nanoparticles. The main Raman peaks for S2 sample are observed at 333 and 371 cm⁻¹, indicating the phase of CZTS nanocrystals without any impurities related to the binary (i.e. SnS_2 (314 and

215 cm^{-1}), Cu$_{2-x}$S (264 and 475 cm^{-1}), and ZnS (275 and 352 cm^{-1})), and ternary phases (i.e. Cu$_2$SnS$_3$ (Tetragonal, 297, 337 and 352 cm^{-1})) [9, 10].
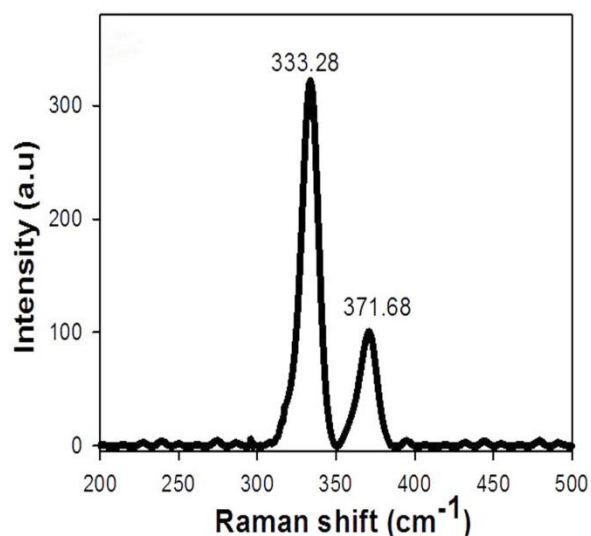

Figure 2. Raman spectrum of WZ CZTS nanoparticles synthesized at 220 ℃ (S2).

Although the mechanism of the formation of CZTS wurtzite phase has been discussed before [9-13], the formation process is not yet fully known. However, we believe that in solution-based synthesis, diffusion controlling or reaction controlling could determine the ionicity of the chemical bonds prevailed during the reaction. Regulacio et al. [13] believed that the types of solvent and capping ligand play key roles in determining the CZTS phase structure. They reported that once the initially formed nuclei of binary zinc sulfide Cu$_{1.8}$S with the structure of cubic close packing (ccp) array of sulfur anions are produced, the final formed phase of CZTS would also be kesterite. However, when the initial nuclei of Cu$_{1.94}$S with the structure of hexagonal close-packed (hcp) anionic framework are produced, the final phase of CZTS would be wurtzite. They also found that using a combination of two solvents in the synthesis process and simultaneous synthesis of the initial nuclei of both Cu$_{1.8}$S and Cu$_{1.94}$S in the medium would result in a combination of both phases of kesterite and wurtzite as the final product. We believe that the formation of

one of the two phases of kesterite and wurtzite in reaction medium is always a competition due to the formation of various binary composites of copper sulfide with different phases, depending on the used concentrations of precursors, solvent, sulfur source, and the capping ligand. However, there is a tendency toward the thermodynamically stable state (in descending order as kesterite>stannite>WZ-kesterite>WZ stannite) regardless of the effective chemical factors. In most reports, structure formation tends toward the more stable state (kesterite) in the synthesis via various methods [1-5, 8, 14]. On the other hand, with the introduction of chemical parameters affecting the reaction rate and kineticsand the formation of the majority of the initial nuclei with a structure near to wurtzite, there is a more tendency towards the formation of wurtzite structure. Occasionally in the formation of structure, a dual and close competition occurs between copper sulfide nuclei with cubic and monoclinic structures, leading to the formation of wurtzite structure, with the particles tending to grow along the preferred and more stable directions of (112) or (002). Through his hard-soft acid-base theory, Pearson [18] reported that Cu$^+$, Zn^{2+}, and Sn^{4+} are soft, intermediate, and hard Lewis acids, respectively. According to this theory, these nucleophilic reagents (Lewis bases) should be in the reactivity order as Cu$^+$ > Zn^{2+} > Sn^{4+}. However, this order could be altered for two reasons: (i) the coordination of capping ligands in the reaction system and (ii) the preferential formation of ternary Cu-Sn-S compound, which may lower the thermodynamic energy of the reaction, causing the reaction between Sn and S proceeds faster than the reaction between Zn and S [15]. Based on these reasons and the findings of Zou et al. [15], when reaction rate between metal precursor and S source is low, the nuclei are Sn-rich and create the zinc blend-derived kesterite structure, while in a fast reaction the nuclei

Shadrokh, Yazdani and Eshghi

are Cu- and Zn-rich, so the WZ structure is formed. Moreover, analysis of EDS data of S1 and S2 samples reveals the atomic percentages of Cu/Zn/Sn/S as 28.68/18.76/18.63/33.9 and 24.70/12.05/11.6/51.56, for S1 and S2, respectively. Based on these results and the above-mentioned reasons, it is clear that S1 is S-poor but S2 is closer to the stoichiometric ratio of CZTS and is slightly Zn- and Cu-rich, hence as temperature increases, the rate of reaction between S with Zn and Cu increases, leading to the formation of Cu- and Zn-rich nuclei and consequently the WZ phase. Reaction temperature, as an effective thermodynamic parameter, is capable of changing the reaction kinetics, nucleation rate, nanoparticles' growth, and reactivity of precursors. Zou et al. [15] reported that $ZnCl_2$, due to its strong complexation between chloride and zinc ions, should be less reactive than $Zn(Ac)_2$. In conclusion, by using $M(Ac)_2$ (M= Cu and Zn), TU and PVP, it seems that the high reactivity between Zn and S at a suitable temperature leads to the formation of pure WZ CZTS nuclei, regardless of the rate of reaction between Cu and S. As a result, the change of reactivity of $Zn(Ac)_2$ in the presence of PVP and EG is an important parameter for the phase-controllable synthesis of WZ CZTS nanocrystals in our experiments. Thus, there is a need for the increased reactivity of Zn precursor (zinc acetate) for the formation of WZ CZTS nanocrystals. In comparison, we have synthesized kesterite structure of spherical CZTS nanoparticles using metal chloride, TU, EG, and PVP as capping ligands via a solvothermal method [14]. We showed that the substitution of metal acetate salts of Zn and Cu with their metal chloride salts leads to the formation of WZ structure of CZTS. Figure 3 presents the FESEM images of CZTS nanocrystals within samples S1 and S2. It is observed that the sphere-like nanoparticles of S1 are aggregated with an average particle size of 30-60 nm. As a

result, the flower-like nanoparticles of S2 are produced from the aggregation of sheet-like nanoparticles. In this regard, PVP and reaction temperature are found as effective parameters on morphological changes, nucleation extent, and growth rate of CZTS nanoparticles. Besides, different morphologies might be developed because of different rates of PVP adsorption on the surface of nanoparticles at two different temperatures. Zhou et al. [8] reported that PVP can be selectively adsorbed on some facets of CZTS crystals, where the growth rates of these facets could be controlled kinetically.
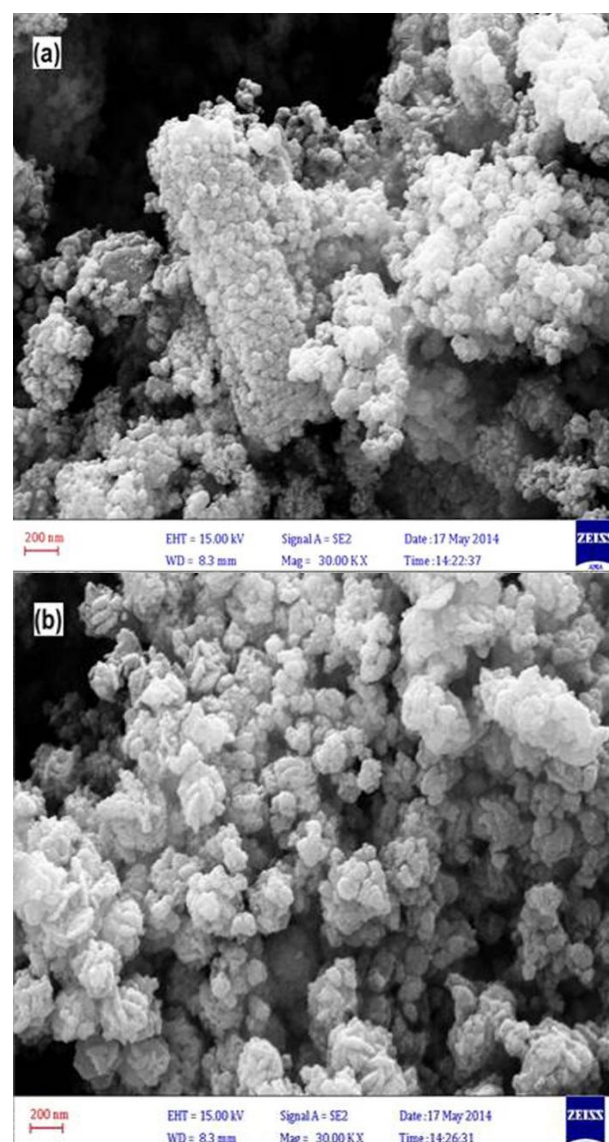

Figure 3. *FESEM images of (a) S1 and (b) S2 WZ CZTS nanoparticles.*

Figure 4 presents the optical absorption spectra of WZ CZTS nanocrystals dispersed in ethanol, and the optical band gaps of S1 and S2 determined by plotting $(Ah\nu)^2$ versus $h\nu$ (where A is absorbance, h is Plank's constant, and ν is frequency of incident light).

The absorption spectra of WZ CZTS nanocrystals show a broad absorption in the visible region of light and a tail extending to the longer wavelengths. Absorption shoulder peaks at 550 nm (2.25 eV) and 500 nm (2.48 eV), which could be related to the excitonic peaks, are observed for S1 and S2 samples, respectively. Bandgap values for S1 and S2 nanoparticles were obtained as 1.45 eV and 1.28 eV, respectively. Note that the band gap energy is strongly controlled by the particle size (quantum confinement). Moreover, the bandgap values of S1 and S2 are relatively close to those reported in previous works (1.2-1.5 eV), indicating their suitability for the photovoltaic applications.

WZ CZTS powder was dispersed in ethanol (5 mg/ml) and drop casted onto 10×20 mm glass substrates. The thin films were annealed at 500 ℃ (5 ℃/min) in Ar flow for 30 min. Electrical contacts consisted of fine copper wire attached to the crystals (10 mm×10 mm) with silver paste. Samples were placed under vacuum conditions for 24 h in order to allow the silver paste to dry completely, leading to the improved contact performance.

I–V curves were measured to analyze the optoelectronic properties of WZ CZTS thin films, as shown in Fig. 5. The figure shows that current through the as-deposited thin film was very weak (which was 1.29 μA for 4 V bias). But after annealing, the current significantly increased due to the decrease in resistivity [19].

The currents of the annealed WZ CZTS thin films for a 4 V bias were 75.88μA in dark and 97.69 μA under illumination (100mWcm^{-2}, Xenon Lamp), confirming that the resistivity of WZ CZTS thin films was decreased under illumination due to
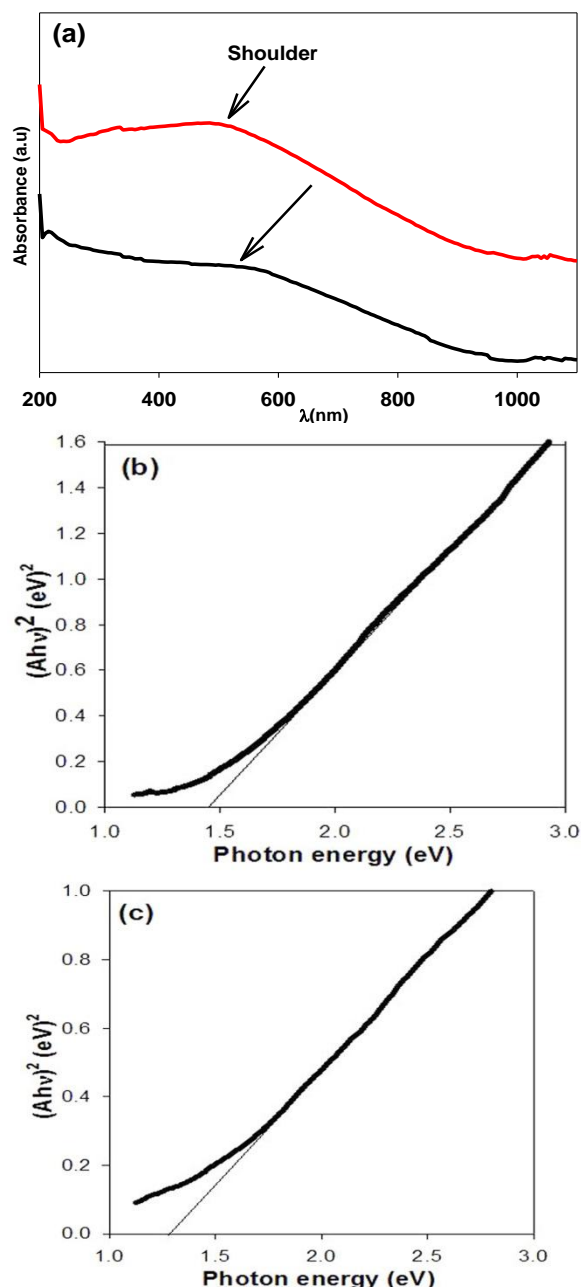

Figure 4. (a) UV-Vis absorption spectra of S1 (black) and S2 (red) powder dispersed in ethanol, and (b) and (c) plots of $(Ah\nu)^2$ vs. $h\nu$ for estimation of optical band gaps of S1 and S2, respectively.

the photo-induced increase of charge carrier [12], which implies its potential for photovoltaic applications.

4. CONCLUSION

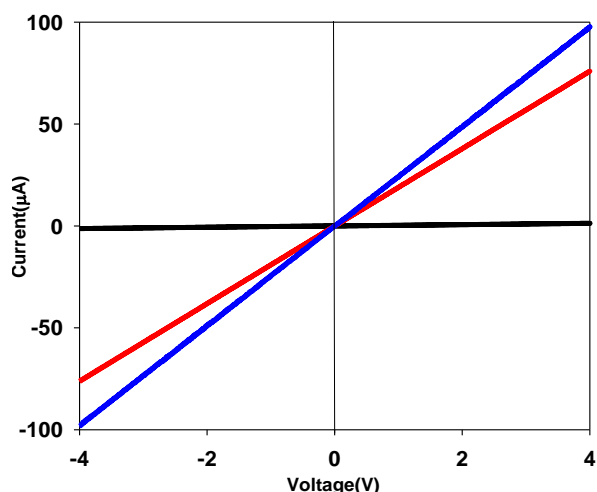In the present work, the temperature and zinc acetate were determined as the key

Figure 5. *I-V curves of as-deposited WZ-CZTS thin film (black), annealed thin film in dark (red), and annealed thin film under illumination (blue).*

parameters in the formation of hexagonal wurtzite structure of CZTS via a low-cost and simple solvothermal method. As zinc acetate was used, WZ phase of CZTS was formed because of the increased reaction rate between Zn and S sources. In addition, the importance of the increased reactivity of Zn precursor for the formation of WZ CZTS was confirmed in the present work. As the reaction temperature rises to 220 ℃, higher crystallinity without any impurities and larger particles' size were obtained. WZ-CZTS particles with a metastable structure had an optical bandgap of 1.45 eV and a favorable photoresponse, which make them promising candidates for thin-film solar cells.

REFERENCES

1. Riha Sh C., Parkinson B A., Prieto A L., (2009). "Solution-Based Synthesis and Characterization of Cu_2ZnSnS_4 Nanocrystals" *J Am Chem Soc.,* 131: 12054-12055.
2. Guo Q., Hillhouse H W., Agrawal R. , (2009). "Synthesis of Cu_2ZnSnS_4 Nanocrystal Ink and Its Use for Solar Cells" *J Am Chem Soc.*, 131: 11672-11673.
3. Tanaka K., Oonuki M., Moritake N., Uchiki H., (2009). " Cu_2ZnSnS_4 thin film solar cells prepared by non-vacuum processing" *Solar Energy Materials & Solar Cells*, 93: 583-587.
4. Gu, E., Yan, C., Liu, F., Liu, Y., Su, Z., Zhang, K and Liu, Y. (2015). "Cu_2ZnSnS_4 thin film solar cells from coated nanocrystals ink" *Journal of Materials Science: Materials in Electronics*, 26: 1932-1939.
5. Wei M., Du Q., Wang D., Liu W., Jiang G., Zhu Ch., (2012). "Synthesis of spindle-like kesterite Cu_2ZnSnS_4 nanoparticles using thiorea as sulfur source" *Materials Letters*, 79: 177-179.
6. Yan X., Michael E., Komarneni S., Brownson J R., Yan ZF., (2014). "Microwave-hydrothermal/solvothermal synthesis of kesterite, an emerging photovoltaic material" *Ceramics International*, 40: 1985-1992.
7. Park J., Song M., Jung W M., Lee W Y., Kim H., Kim Y., Hwang Ch., Shim IW., (2013). "Syntheses of Cu_2SnS_3 and Cu_2ZnSnS_4 nanoparticles with tunable Zn/Sn ratios under multibubble sonolumine scence conditions*" Dalton Trans*, 42: 10545-10551.
8. Zhou YL., Zhou WH., Du YF., Li M., Wu SX., (2011). "Hierarchical Cu_2ZnSnS_4 Particles for a Low-Cost Solar Cell: Morphology Control and Growth Mechanism"*J. Phys. Chem. C*, 115: 19632-19639.
9. Singh A., Geaney H., Laffir F., Ryan K M., (2012). "Colloidal Synthesis of Wurtzite Cu_2ZnSnS_4 Nanorods and Their Perpendicular Assembly" *J. Am. Chem. Soc.,* 134: 2910-2913.
10. Li Y., Han Q., Kim T W., Shi W., (2014). "Synthesis of Wurtzite - Zincblende Cu_2ZnSnS_4 and $Cu_2ZnSnSe_4$ Nanocrystals: Insight into the Structural Selection of Quaternary and Ternary Compounds influenced by Binary nucleus" *Nanoscale*, 6: 3777-3786.
11. Lu X., Zhuang Z., Peng Q., Li Y., (2011)." Wurtzite Cu_2ZnSnS_4 nanocrystals: a novel quaternary semiconductor" *Commun,* 47: 3141-3143.
12. Kang Ch-Ch., Chen H-F, Yu T-Ch, Lin T-Ch, (2013). "Aqueous synthesis of wurtzite Cu_2ZnSnS_4 nanocrystals" *Materials Letters*, 96, 24-26.
13. Regulacio M D., Ye Ch., Lim S H., Bosman M, Ye E., Chen Sh., Xu Q H., Han M Y., (2012). "Colloidal Nanocrystals of Wurtzite-Type Cu_2ZnSnS_4: Facile Noninjection Synthesis and Formation Mechanism" *Chem. Eur. J.*, 18: 3127-1331.
14. Shadrokh Z., Eshghi H., Yazdani A., (2015). "Investigating the effects of temperature and metal ion ratio on physical and optical properties of Cu_2ZnSnS_4 nanoparticles and thin films" *Materials Science in Semiconductor Processing*, 40: 752-758.
15. Zou Y., Su X., Jiang J., (2013). "Phase-controlled synthesis of Cu_2ZnSnS_4 nanocrystals: the role of reactivity between Zn and S" *J. Am. Chem. Soc.*, 135: 18377-18384.

16. Luo Q., Zeng Y., Chen L., Ma Ch., (2014). "Controllable Synthesis of Wurtzite Cu_2ZnSnS_4 Nanocrystals by Hot-Injection Approach and Growth Mechanism Studies*" Chem. Asian J.*, 9: 2309-2316.
17. Sarswat P. K, Free M. L., (2013). "An investigation of rapidly synthesized Cu_2ZnSnS_4 nanocrystals" *Journal of Crystal Growth*, 372: 87-94.
18. Pearson R.C., (1963) "Hard and Soft Acids and Bases" *J. Am. Chem. Soc.*, 85: 3533-2539.
19. Tanaka K., Oonuki M., Moritake N., Uchiki H., (2009). "Cu_2ZnSnS_4 thin film solar cells prepared by non-vacuum processing" *Solar Energy Materials & Solar Cells,* 93: 583-587.